NUMERICAL SIMULATION OF MAGNICON AMPLIFIER

V.Yakovlev, O.Danilov, O.Nezhevenko, V.Tarnetsky, Budker INP, Russia

I. INTRODUCTION

Magnicon is a new RF source with the round beam deflection [1,2]. The main features of this device are high efficiency and reduced sensitivity to variations in load impedance. Those features make magnicon to be attractive for accelerator applications. Magnicon may be designed as an amplifier and as a frequency multiplier. Magnicon with the frequency multiplication in centimeter wave range may turn into one of main RF sources for future linear colliders.

Magnicon theory is developed for ideal RF field and for small deflecting angles of infinitely thin electron beam [3]. But large deflecting angle and, thus, large beam tunnel apertures are necessary for power generating of tens and hundreds of MW. Fringing fields of the beam tunnels, RF-field non-linearity far from the cavity axis and finite beam diameter lead not only to quantitative perturbations of device parameters, but change the process of beam-cavity interaction in principle [4,5]. It is necessary to take into account all mentioned phenomena to build a working device.

We have developed methods and computer codes for particle simulations of the beam-cavity interaction in magnicon employing the realistic DC magnetic and RF fields and finite beam diameter. Computer simulation codes presented in this report does not treat electron gun problems, which are described in details in [6].

II. PHYSICAL MODEL

We developed the two models for magnicon analysis to find a working version providing optimal efficiency:

a. the steady-state model;

b. the time-depended one.

The steady-state model employs fixed amplitudes and phases of RF-fields in magnicon cavities. Self-consistency is achieved by iteration until power balance takes place in each cavity (i.e. until the beam energy loss equals to energy dissipation in the cavity wall or in the load). Dominance of the beam energy loss in the cavity in the absence of preliminary beam deflecting indicates the self-excitation on the working frequency [4]. Longitudinal DC magnetic field is formed by the magnetic system, which includes not only separate coils with independent current supplies, but magnetic shields having relevant configuration [3]. In our model we use the field calculated for real magnetic system without taking into account iron saturation, which are negligible in our case because of small field value [6]. We use for calculations the realistic rotating RF-fields of the cavities connected by beam tunnels to take into account influence of the fringing field. The resonance frequency of a cavity may be multiple of the drive frequency with corresponding azimuthal number. The simulations propagate an electron beam through a sequence of deflection cavities and an output cavity. We use $2\frac{1}{2}D$ macroparticle model of the beam without space charge. To estimate influence of the space charge scalloped beam is considered with arbitrary value of the cathode magnetic field. The simulation may be carried out by following a single temporal slice because of phase synchronism. During calculations of the beam dynamics in the fixed fields the beam power losses and the cavities detuning caused by the beam are calculated. When the self-consistent solution is found, it is necessary to produce its stability test, because the regime obtained as a result of optimizing may be unstable both in the deflecting system and in the output cavity. In the deflecting system this instability may have a view of RF field amplitude jump lead to the cavity breakdown [10]. In the case of instability in the output cavity the regime of small efficiency may be realized. For stability analysis Lyapunov's method is used: differential equations for RF field amplitude growth in the cavity are linearized near the working point in amplitude-phase coordinates. The resulting system of the linear equations is used for determination of the instability growth rate.

After magnicon optimizing by the steady-state code and stability test, we use the time dependent model to calculate duration and type of a transient process of magnicon excitation. Time dependent simulation is fulfilled based on slow amplitude approximation of the differential equations for RF field complex amplitudes. During each step of numerical integration of those equations it is necessary to calculate complex power of the beam losses, and thus, to solve the steady-state problem.

III. COMPUTER MODELS

a. Axial DC magnetic field is calculated using SAM code [7] for a real geometry of the magnetic system in linear approximation. In this case we solve N magnetostatic problems (N is the number of coils in the magnetic system). When we solve the i-th problem, we assume the current in the i-th coil to be unit, and in another coils to be zero. The total field is calculated as a superposition when all the coil currents are distributed previously. It gives the possibility of operative changes of the coil currents during the beam dynamics calculations.

b. The cavity RF-field is calculated by the next way [8]: the resonance frequency and Hr and Hz components are calculated by SUPERLANS2 code [9] for arbitrary azimuthal wave number m. The azimuthal component H_φ is determined using the next equation:

$$\Delta H_\varphi - \frac{H_\varphi}{r^2} + \left(\frac{\omega}{c}\right)^2 H_\varphi = \frac{2m}{r^2} H_r \qquad (1)$$

where ω is the resonance frequency, c is speed of light. The calculating error does not increase because of smoothing properties of Laplace operator. But it is not possible to use the electric field calculated by numerical derivation because of unacceptably large errors. We calculate the current surface distribution using the magnetic field calculated by

SUPERLANS2 and then find the RF-field in arbitrary point integrating the surface source field over the cavity boundary [8]. For the approximation of the surface current distribution, we use a third-order spline fit. In this case, all six field components will satisfy Maxwell equations and we have the same precision of calculations. To reduce the RF field calculation time inside the cavity, we use paraxial field expansion. We have found an analytical formula for arbitrary-order paraxial expansion of the surface source fields of arbitrary azimuthal dependence. The longitudinal dependences of paraxial expansion coefficients are approximated by a third-order spline. It is possible to calculate the excitation of several modes in the same cavity. The maximal surface electric field is calculated and displayed for electric strength analysis of the cavity working in investigating regime.

c. For integration of macroparticle equations of motions a third-order Runge-Kutta method is used. Simultaneously we integrate the complex electric field along the trajectory to find the complex power loss of macroparticle. The total beam power loss P is determined by sum of the power losses over all macroparticles. Imaginary part of the beam power loss determines the cavity detuning caused by the beam:

$$\Delta\omega = \frac{\mathrm{Im}(P)}{w} \tag{2}$$

where w is the energy stored in the cavity. The beam kinetic energy changes in process of deflection and deceleration in the output cavity and real part of the total beam power loss are used to check the calculation precision. Thirty-seven macroparticles are typically employed, but up to 177 macroparticles are used to verify the accuracy of the final simulations.

d. For stability analysis we use the next equations for the RF-field amplitude u_i and phase φ_i in i-th cavity:

$$\frac{du_i}{dt} = -\frac{u_i}{\tau_i}\left(1-\frac{\mathrm{Re}(P_i)}{P_{id}}\right) \tag{3}$$
$$\frac{d\varphi_i}{dt} = \delta\,\omega_i + \frac{\mathrm{Im}(P_i)}{w_i}$$

where P_{id} is power dissipation in the cavity wall (or in the load), τ_i is the time constant, $\delta\omega_i$ is the difference between the cavity resonance frequency and the working frequency. Then we produce linearizing of (3) near the stationary point, the derivatives of right-hand side of (3) we find numerically, solving the steady-state problems with perturbed amplitude and phase. Eigen values of the matrix of the linear system are equal to the instability growth rates.

e. For time-depended simulations we use the same system of equations (3) for all cavities excluding the first one, where the field is determined by the drive power. This system is integrated using the third-order Runge-Kutta method. One should notice that the system (3) is stiff because the time constant of the output cavity is much less than the time constants for deflecting cavities. Thus, we plan to use an implicit method to solve (3) to decrease the calculation time.

IV. THE COMPUTER CODES

We have designed the computer codes for magnicon simulations for PC and VAX based on the methods described above. Because it is necessary to make calculation of considerably large number of variants during magnicon optimizing, and the number of input parameters is large too, friendly user's interface with graphics is needed for effective work with the codes. The dialogue used in those codes is based on menu system and table input/output of symbol information. Mouse is used for an output data processing in the graphic window directly. The final document containing the total input and output information with graphics is prepared automatically as a result of the code run.

V. EXAMPLES

In the Fig.1 there are the results of calculation of the 7 GHz frequency doubling magnicon having the beam power of 100 MW [4,6]. The beam voltage is 430 kV, the beam current is 230 A. Calculated efficiency for this version is 54%. The trajectories of 37 macroparticles in (r,z) coordinates are shown as well as longitudinal dependence of the energy of each macroparticle. The longitudinal distribution of axial DC magnetic field is shown in the Fig. 2. Fig. 3 shows the field map of the operating mode of the penultimate cavity. The transient processes of amplitude growth in all cavities are shown in Fig. 4. The bold curve corresponds to the process in the output cavity. Fig. 5 illustrates an unstable (for the output cavity) transient process in the output cavity for one of the regimes with small efficiency.

VI. SUMMARY

Simulation model and computer codes are developed for calculation of the fields and the beam dynamics in magnicon taking into account beam tunnel fringing field and finite beam diameter. Those codes were used in investigations of physical processes in magnicon and helped to develop the first operating magnicon design [10] and it's improved version, which is under fabrication.

VII. REFERENCES

[1] M.M.Karliner, *et al.*,"The magnicon- An advanced version of the gyrocon", Nucl. Instrum. Methods Phys. Res.,vol. A269,pp. 459-473,1988.

[2] O.A.Nezhevenko,"The magnicon: A new RF power source for accelerators", in IEEE Particle Accelerator Conf. Rec., 1991, vol.5, pp. 2933-2942..

[3] M.M.Karliner, E.V.Kozyrev, A.Yu.Maximov, O.A.Nezhevenko, "An approximate theory of the magnicon", Preprint INP 88-64, Novosibirsk, 1988 (in Russian).

[4] O.Nezhevenko, "Gyrocons and magnicons: microwave generators with circular deflection of the electron beam", IEEE Trans. on Plasma Science, vol. 22, pp. 756-772, 1994.

[5] O.Nezhevenko, *et al.*, "First test of the X-band pulsed magnicon", in Proc. IEEE Particle Accelerator Conf., 1993, vol.4, pp. 2650-2652.

[6] Y.V.Baryshev, *et al.*, "Electron optic system for forming 100 MW beam with high current density and microsecond pulse duration for X-band magnicon", in Proc. 8th Int. Conf. High power Particle Beams, Novosibirsk, Russia, vol. 1, pp. 598-603,1990.

[7] B.M.Fomel, M.A.Tiunov, and V.P.Yakovlev, “Computer-Aided Electron Gun Design”, in Proc . XIII International Conference on High Energy Accelerators, 1987, vol. 1, pp.353-355.

[8] O.A.Nezhevenko, V.P.Yakovlev, S.H.Gold, and B.Hafizi,”Design of a High Power X-Band Magnicon Amplifier”, IEEE Trans. on Plasma Science, vol.22, pp. 785-795 , 1994.

[9] D.G.Myakishev, and V.P.Yakovlev, “The new possibilities of SUPERLANS2 code”, these Proceedings.

[10] I.Zapryagaev *et al.*, “Status of X-Band Pulsed Magnicon”, in Proc. Eur. Particle Accelerator Conf., 1994, vol. 3, pp. 1927.

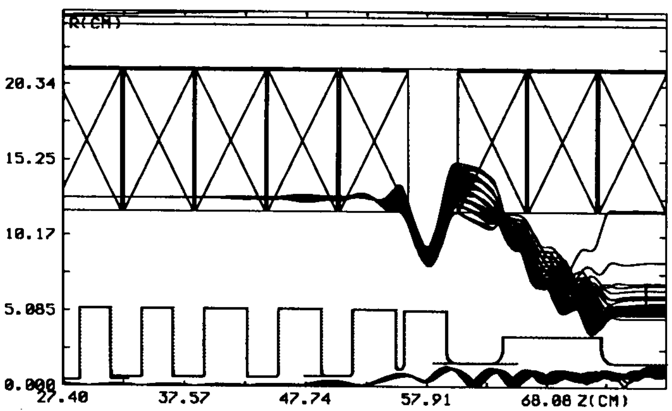

Fig. 1. Steady-state simulation of the magnicon design with the efficiency of 54%.

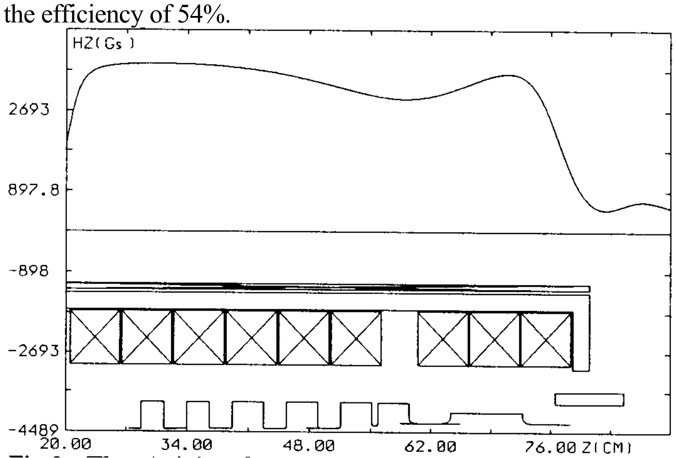

Fig.2. The Axial DC magnetic field profile used in the simulations.

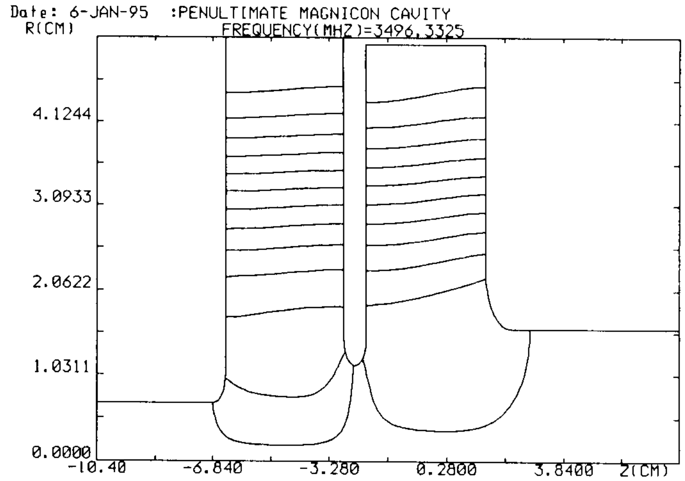

Fig. 3. The field map of the operating mode in the penultimate cavity.

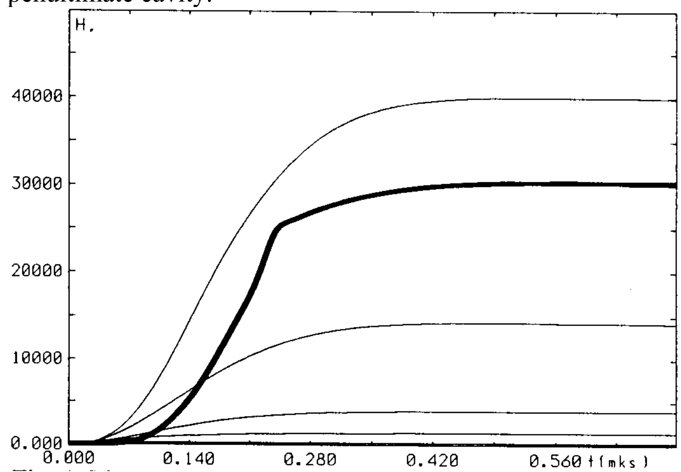

Fig. 4. The transient process in the magnicon.

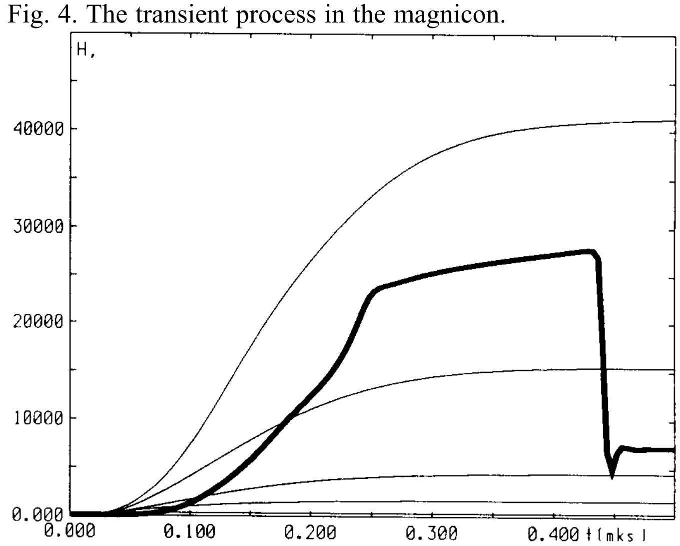

Fig.5. The unstabe regime of the output cavity excitation.